Carbon-Supported Platinum Catalyst Electrodes: Characterization by Transmission Electron Microscopy, X-ray Absorption Spectroscopy, and Electrochemical Half-Cell Measurement on a P...

ARTICLE *in* THE JOURNAL OF PHYSICAL CHEMISTRY · OCTOBER 1995

Impact Factor: 2.78 · DOI: 10.1021/j100040a033

4 AUTHORS, INCLUDING:

Chang Jen-Ray
National Chung Cheng University
56 PUBLICATIONS **949** CITATIONS

Carbon-Supported Platinum Catalyst Electrodes: Characterization by Transmission Electron Microscopy, X-ray Absorption Spectroscopy, and Electrochemical Half-Cell Measurement on a Phosphoric Acid Fuel Cell

J.-R. Chang

Department of Chemical Engineering, National Chung Cheng University, Chia-Yi, Taiwan, R.O.C.

J.-F. Lee

Synchrotron Radiation Research Center, No.1, R&D Road VI, Hsinchu, Taiwan, R.O.C.

S. D. Lin

Department of Chemical Engineering, Yuan-Ze Institute of Technology, Neili, Taiwan, R.O.C.

A. S. Lin*

Energy and Resource Laboratories, Industrial Technology Research Institute, Hsinchu, Taiwan, R.O.C.

Received: April 18, 1995; In Final Form: July 22, 1995[⊗]

An electrode for a phosphoric acid fuel cell (PAFC) was prepared by the deposition of carbon-supported platinum catalysts on a PTFE (Polytetrafluoroethylene)-treated carbon paper, followed by a passivation in flowing nitrogen at 300 °C. The electrode performance was tested in phosphoric acid electrolyte at 190 °C by using a three-electrode half-cell system with either a Pd/H or a dynamic hydrogen reference electrode. The structure of platinum clusters on the catalyst powders, the fresh electrode, and the electrode after six test cycles was characterized by transmission electron microscopy (TEM) and X-ray absorption spectroscopy. Both the catalyst powders and the fresh electrode have the same white line intensity and extended X-ray absorption fine structure (EXAFS) on the Pt L_{III} edge, indicating that the morphology and electric properties of the platinum clusters were not altered during electrode fabrication. However, after the electrochemical tests, some of the platinum clusters on the electrode were aggregated. The average Pt−Pt coordination number in the Pt clusters increased from 5.5 to 6.1 while no change in the Pt−Pt bond distance (2.77 Å) was observed. TEM analysis also shows an increase in the average Pt particle size from 32 to 45 Å and a broadening in particle size distribution when comparing the fresh catalyst with the Pt-containing powders scraped off from the used electrode. In addition, a slight decrease in the normalized white line intensity characterizing the Pt clusters on the electrode was observed after the electrochemical tests. The decrease in the white line intensity could be due to a growth of Pt clusters and/or a reduction of partially oxidized Pt clusters on the electrode during the electrochemical tests.

Introduction

The carbon-supported noble metal electrocatalyst on a porous gas diffusion electrode is a critical component for an individual single cell and an entire cell stack of phosphoric acid fuel cells (PAFC); platinum is the most commonly used noble metal in these catalysts. The electrode performance and durability can be determined by a number of parameters, e.g., corrosion of carbon, electrode morphology, electrode wettability, and the morphology and crystalline orientation of the noble metal particles in the catalysts.[1−3] Although the influences of these parameters have been studied for many years and the commercial-scale PAFC power plant has advanced to about 200 kW on-site, progress in improving the durability and reliability of the fuel cell stack is still relatively slow.

The performance of a phosphoric acid fuel cell can be evaluated with a half-cell test involving an oxygen reduction reaction over the porous gas diffusion electrode. Among the parameters affecting the performance and durability, the morphology of noble metal clusters in the electrocatalyst is considered to play an important role; however, only limited information regarding this morphological effect was reported in the literature. The inadequacy of this morphological study and the consequent tardiness in improving PAFC performance are probably due to the complexity of the reaction system and the difficulty in the characterization of the morphology of metal clusters in the electrocatalysts.

The extended X-ray absorption fine structure (EXAFS) technique has been shown to be useful for quantitative characterization of the metal morphology for supported metal catalysts.[4−8] Complementary information of metal cluster morphology can also be obtained with transmission electron microscopy (TEM). Thus, combined analyses with both EXAFS and TEM techniques have helped researchers to clarify issues like structure sensitivity over supported metal catalysts.[9,10] In this paper, we report the use of these two techniques to characterize the morphology change of carbon-supported platinum clusters of a phosphoric acid fuel cell during the electrode fabrication process and electrocatalytic reaction. By this, the concern of structure-dependent electrochemical activity is expected to be clarified, and the result would provide information about ways for prolonging electrode durability.

* To whom correspondence should be addressed.

[⊗] Abstract published in *Advance ACS Abstracts,* September 1, 1995.

0022-3654/95/2099-14798$09.00/0

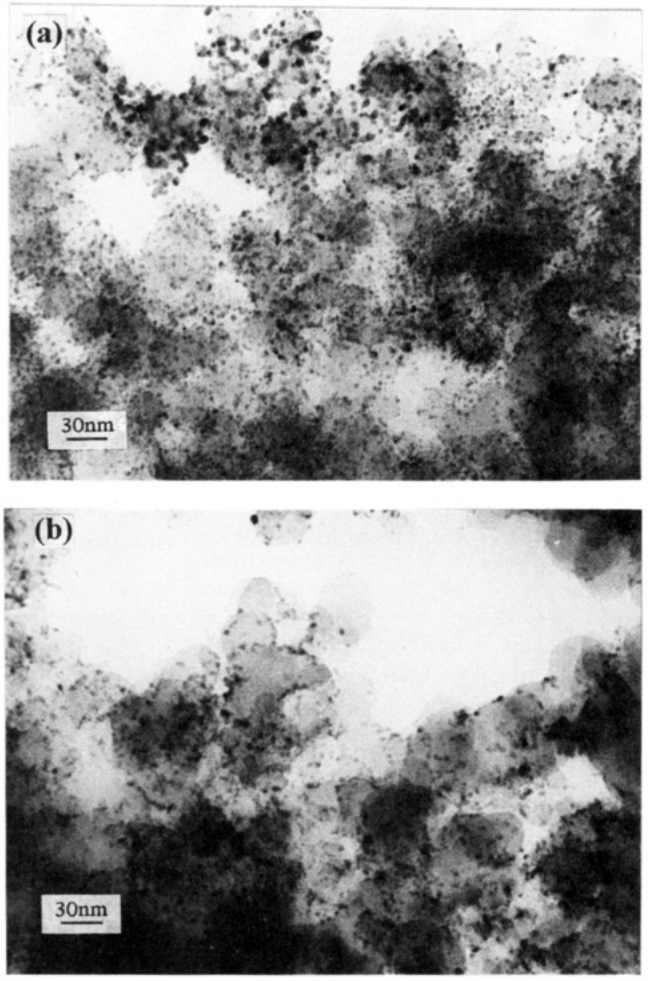

Figure 1. TEM photographs (×100k) of (a) catalysts on the fresh electrode and (b) catalysts on the used electrode; TEM was operated at 160 kV. (The original photograph has been reproduced to 54% of its original size for publication purposes.)

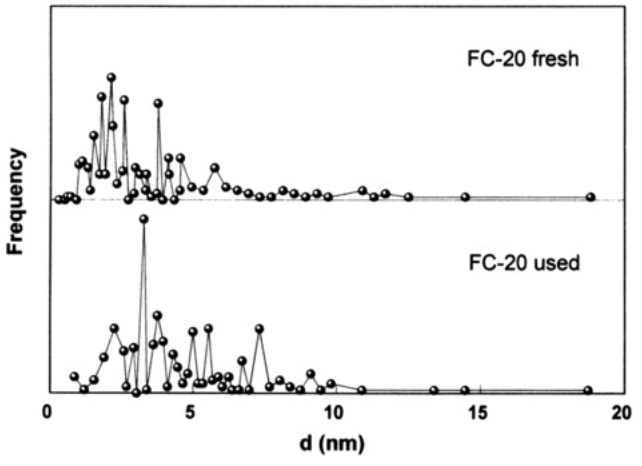

Figure 2. Particle size distribution of Pt clusters on both fresh and used electrodes based on the TEM photographs shown in Figure 1.

Experimental Section

Electrode Preparation. A commercially available carbon-supported Pt catalyst (Johnson Matthey, FC-20) was used for electrode fabrication; the nominal Pt loading is 20 wt %, and the electrochemical metal area is 70−150 m^2/g. The electrodes were prepared from PTFE (polytetrafluoroethylene)-treated carbon paper with a catalyst overlayer. The catalyst layer was prepared from Pt/C catalysts and a PTFE solution to have a Pt loading less than 0.5 mg/cm^2. Then electrodes were dried and sintered at 300 °C before the electrochemical measurement. Details of the electrode fabrication process are given elsewhere.[11]

TABLE 1: Crystallographic Data Characterizing the Reference Compounds and Fourier Transform Ranges Used in the EXAFS Analysis[a]

	crystallographic data			Fourier transform		
sample	shell	N	R, Å	Δk, $Å^{-1}$	Δr, Å	n
Pt soil	Pt−Pt[b]	12	2.77	1.9−19.8	1.9−3.0	3
$Na_2Pt(OH)_6$	Pt−Oc	6	2.05	1.4−17.7	0.5−2.0	3

[a] Notation: N, coordination number for absorber−backscatterer pair; R, absorber−backscatterer distance; Δk, limits used for forward Fourier transformation; Δr, limits used for shell isolation (r is distance); n, power of k used for Fourier transformation. [b] Crystal structure data from Wyckoff, R. W. G. *Crystal Structure*, 2nd ed.; Wiley: New York, 1963; Vol. I, p 10. [c] Crystal structure data from Trömel, M.; Lupprich, E. Z. *Anorg. Chem.* **1975**, *414*, 60.

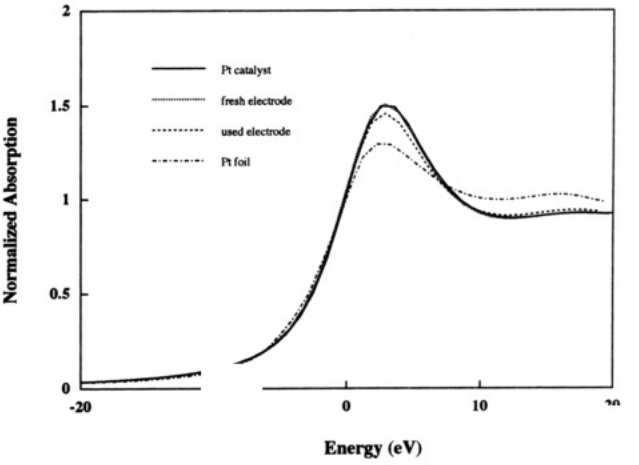

Figure 3. Structure of the Pt L_{III} absorption edge for the carbon-supported Pt catalysts purchased from Johnson Matthey (solid line), the fresh electrode prepared from the Pt catalysts (dotted line), the used electrode: fresh electrode after six electrochemical measurement cycles (dashed line), and the Pt foil reference (dashed−dotted line).

Electrode Performance Test. Electrochemical tests were run by using a three-electrode half-cell system to obtain voltage output as a function of current decay. Phosphoric acid is used as the electrolyte, and the cell is operated at 190 °C. Either a dynamic hydrogen electrode or a Pd/H electrode was used as the reference. Oxygen is supplied to carbon-paper side of the electrode, and a current is applied to the electrode to measure the corresponding potential. Cyclic voltametry and Tafel plots are used to evaluate the electrochemically active area of Pt and the cathodic activity of the electrodes.

Transmission Electron Microscopy. The catalyst layer on the used electrode was scraped off carefully, washed thoroughly with deionized water, and then dried. This catalyst as well as the fresh catalyst is ultrasonically dispersed in ethanol, fetched on Cu grids, and then dried for later TEM analysis. The TEM (JOEL, 200CX) is typically operated at 160 keV.

X-ray Absorption Spectroscopy. The X-ray absorption measurements were performed on X-ray beam line X-11A of the National Synchrotron Light Source (NSLS) at Brookhaven National Laboratory with a storage ring energy of 2.5 GeV and a beam current between 100 and 200 mA. A Si(111) double-crystal monochromator was used for energy selection, and it was detuned 20% at E_0 + 50 eV to suppress higher harmonic radiation; resolution, $\Delta E/E$, was estimated to be 2.0×10^{-4}. The transmission measurement geometry was arranged by using gas-filled ionization chambers to monitor the intensities of the incident and transmitted X-rays. To gain the proper absorption

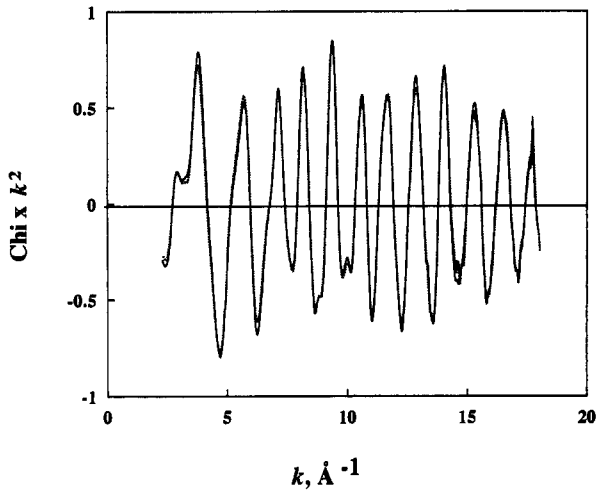

Figure 4. k^2-weighted raw EXAFS data for the carbon-supported Pt catalyst purchased from Johnson Matthey (solid line) and the fresh electrode prepared from the Pt catalyst (dotted line).

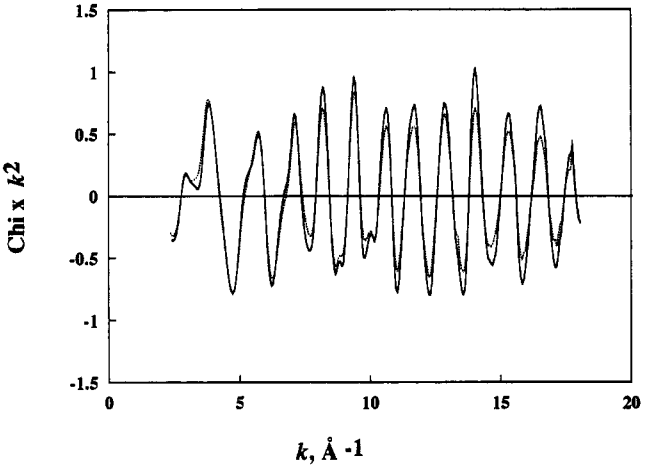

Figure 5. k^2-weighted raw EXAFS data for the fresh electrode (dotted line) and the used electrode (solid line).

ratio for the incoming X-rays, the gas composition in the ionization chamber was selected as argon 3 mL/min with nitrogen 60 mL/min for the first chamber and argon 18 mL/min with nitrogen 24 mL/min for the second chamber, respectively. The monochromator was scanned in energy from 200 eV below the platinum L_{III} absorption edge (11564 eV) to 1200 eV above the edge. The fresh Pt catalysts, fresh electrode, and used electrode were measured respectively in transmission mode at liquid nitrogen temperature. Care was taken to assure good uniformity of the catalyst layer on the electrodes and the measured catalyst samples. A standard Pt foil at room temperature was simultaneously measured as a reference so that energy calibration can be done between scans.

Results and Discussion

Transmission Electron Microscopy. TEM photographs of both the fresh and used catalysts are shown in Figure 1; it shows that the morphology of Pt clusters is somewhat different in these two samples. By counting the clusters' sizes, the Pt particle size distribution was obtained as shown in Figure 2, and a number average particle size of Pt clusters is calculated as 32 and 45 Å, respectively, for fresh and used catalysts. These results show that the used catalysts have a larger average Pt particle size and a wider Pt particle size distribution. This indicates that a growth in Pt clusters occurs during the six cycles of the electrochemical test.

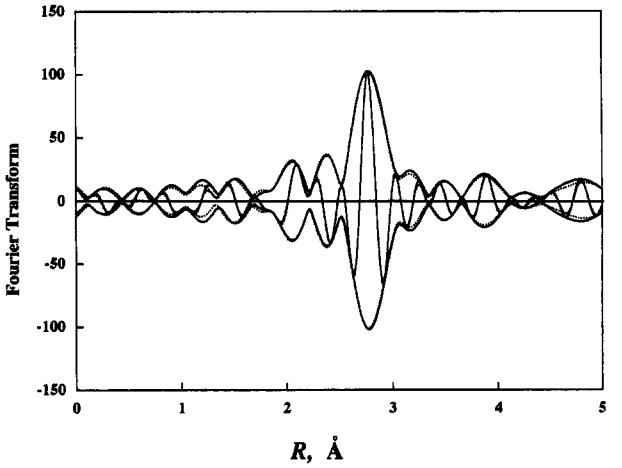

Figure 6. Imaginary part and magnitude of Fourier transform (k^3-weighted, Δk = 3.10−15.0 Å, Pt−Pt phase and amplitude corrected) for the carbon-supported Pt catalysts (solid line) and fresh electrode (dotted line).

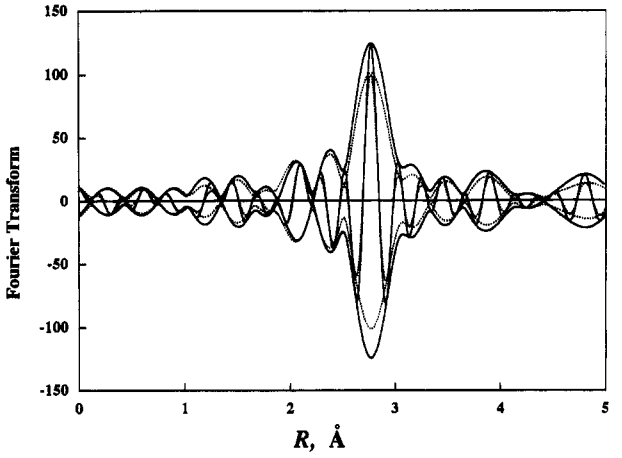

Figure 7. Imaginary part and magnitude of Fourier transform (k^3-weighted, Δk = 3.10−15.0 Å, Pt−Pt phase and amplitude corrected) for the fresh (dotted line) and used electrode (solid line).

EXAFS Reference Data. The EXAFS data were analyzed with experimentally determined reference files obtained from standard materials of known structure (Table 1). The Pt−Pt and Pt−O contributions were analyzed with phase shifts and backscattering amplitudes extracted from EXAFS data for Pt foil and $Na_2Pt(OH)_6$, respectively. These two data files were provided by Dr. B. C. Gates, Department of Chemical Engineering, University of California, Davis. Details of the preparation of the reference files are described elsewhere.[12]

XANES and Preliminary Analysis of EXAFS Data. X-ray absorption data from three scans of each sample were averaged and then the preedge and background were subtracted. Each resulting spectrum was divided by the edge height to obtain the normalized XANES (X-ray absorption near-edge structures) and EXAFS functions. The comparison of XANES spectra for the catalyst powder, fresh electrode, used electrode, and a Pt foil reference is shown in Figure 3, and the comparison of EXAFS spectra for these three samples is shown in Figures 4 and 5. The raw EXAFS data for the samples have a signal to noise ratio >50 (the noise amplitude was determined at k = 14 $Å^{-1}$, and the signal amplitude was determined at k = 4 $Å^{-1}$).

The intensity of the threshold resonance of the L_{III} edge (white line) is related to the transition probability of exciting inner-core 2p electrons into a vacant d valence level. Usually, the lower the electron density of the metal, the greater the number of vacancies in the valence level and, hence, the higher the

TABLE 2: XAFS Results Characterizing the Fresh Electrode Prepared from Carbon Supported Platinum Catalysts by Considering Pt−O as a Low Z Backscattering Contribution[a]

shell	N	R, Å	$\Delta\sigma^2 \times 1000$, Å^2	ΔE_0, eV	EXAFS reference
Pt−Pt	5.51 ± 0.18	2.774 ± 0.002	1.97 ± 0.19	−4.31 ± 0.41	Pt−Pt
Pt−O	2.15 ± 0.10	2.057 ± 0.006	2.85 ± 0.67	2.56 ± 0.87	Pt−O
Pt−Pt	2.49 ± 1.54[b]	3.939 ± 0.049	3.18 ± 4.16	−11.72 ± 7.89	Pt−Pt
Pt−Pt	6.42 ± 2.53[b]	4.814 ± 0.034	2.76 ± 2.91	−5.93 ± 4.55	Pt−Pt

[a] Notes: Z is the atomic number, N the coordination number for absorber−backscatterer pair, R the average absorber−backscatterer distance, $\Delta\sigma^2$ the Debye−Waller factor, and ΔE_0 the inner potential correction. [b] Note:To consider the difference of absorber−backscatterer distance between the reference shell and the higher Pt−Pt shell to be analyzed, the coordination number N of the higher Pt−Pt shell is corrected by the equation, $N=N_{unc}\, e^{2(R_j-R_{ref})/\lambda(k)}$, where N_{unc} is determined in the EXAFS data analysis by using R_{ref} as a reference coordination distance.[12]

TABLE 3: EXAFS Results Characterizing the Used Electrode Prepared from Carbon Supported Platinum Catalysts by Considering Pt−O as a Low Z Backscattering Contribution[a]

shell	N	R, Å	$\Delta\sigma^2 \times 1000$, Å^2	ΔE_0, eV	EXAFS reference
Pt−Pt	6.05 ± 0.16	2.772 ± 0.002	1.45 ± 0.15	−3.26 ± 0.35	Pt−Pt
Pt−O	2.12 ± 0.13	2.052 ± 0.007	4.48 ± 0.84	4.20 ± 1.04	Pt−O
Pt−Pt	2.96 ± 1.38[b]	3.932 ± 0.035	2.62 ± 2.99	−9.63 ± 5.80	Pt−Pt
Pt−Pt	7.58 ± 2.13[b]	4.805 ± 0.023	2.00 ± 1.97	−4.70 ± 3.23	Pt−Pt

[a] All footnotes as in Table 2.

probability of the transition or the higher the white line intensity.[13] A semiquantitative correlation between oxidation state and the intensity of the white line of the supported metal catalyst has been noted by Meitzner et al.[14] and Fung et al.[15] However, the effects of cluster size on the white line intensity must also be considered. Hartree−Fock−Slater LCAO calculations show a decrease in the number of unfilled d states (i.e., a decrease in the white line intensity) with increasing size of ionized clusters as a consequence of the better screening in the larger clusters of the core hole of the ionized atom.[16] The results are consistent with reported XANES data showing that the white line intensity of supported metal clusters decreases with increasing metal particle size.[17]

The near-edge absorption spectra (Figure 3) show that the white line intensity of the fresh electrode sample is very close to that of Pt/C catalyst powder, while the used electrode sample exhibited a white line of slightly lower intensity than the fresh electrode. Among the four samples, the Pt foil reference, however, gives the lowest white line intensity, suggesting that the ionized Pt clusters are present on the catalyst and electrodes. The almost equal intensities for the catalyst powder and the fresh electrode indicate that the change in oxidation state and morphology of Pt clusters owing to electrode fabrication is negligible. In contrast, by considering the effects of cluster size on the white line intensity, the decrease in white line intensity after the electrochemical test was thought to be caused by the growth of the Pt cluster size during the test. However, it may be due also to the reduction of the oxidized Pt during the test, based on the correlation between oxidation state and the intensity of the white line absorbance.

Prior to the detailed EXAFS data analysis, k^3-weighted Pt−Pt phase- and amplitude-corrected Fourier transforms were determined for the EXAFS functions ($4.1 < k < 16.0$). The Fourier transforms provide the qualitative information about the influence of electrode fabrication and electrocatalytic reaction on the structure of the supported Pt clusters. As shown in Figure 6, the Fourier transform peaks of Pt/C catalyst powder and fresh electrode samples are almost identical in both position and intensity. In contrast, the Fourier-transformed EXAFS functions of the fresh and used samples (Figure 7) show that the peaks corresponding to the first metal−metal shell (at about 2.8 Å) and higher shells are also at the same positions, while the peaks for the used electrode are higher than those of the fresh electrode. These results suggest that there was no significant structural change of Pt clusters during the electrode fabrication process and the high temperature (300 °C) passivation process, whereas a remarkable agglomeration of Pt clusters occurred during the electrochemical tests, consistent with the XANES and TEM results.

Detailed EXAFS Analysis. A k^2-weighted Fourier transformation without correction was performed on the EXAFS function over the range $4.17 < k < 17.90$ Å^{-1} for the fresh electrode sample and $4.21 < k < 17.90$ Å^{-1} for the used electrode. The major contributions were isolated by inverse Fourier transformation of the data in the range $1.06 < r < 3.23$ Å for the fresh electrode sample and $1.02 < r < 3.23$ Å for the used electrode. At the beginning, the coarse structural parameters characteristic of the Pt−Pt contribution were determined by fitting the k^2-weighted Fourier-isolated EXAFS function in the range $8.5 < k < 15.0$ Å^{-1}. An EXAFS function calculated from these parameters was then subtracted from the raw data (Fourier isolated EXAFS function). There were no oscillations in the high-k (>10 Å^{-1}) range of the residual spectrum being observed. Therefore, such a residual spectrum was expected to represent the metal−support interactions. A k^3-weighted Pt−O phase-corrected Fourier transformation was thus performed on the residual EXAFS data to examine the EXAFS contributions from the backscattering atoms of low atomic number. The resultant Fourier transform showed only one peak at about 2.1 Å in r space. The structural parameters of this contribution (Pt−O) were then estimated by fitting the k^1-weighted residual data in the range $4.3 < k < 10.5$ Å^{-1}. The Pt−O contribution was subtracted from the raw data, and more accurate parameters for the Pt−Pt contribution can be determined. This procedure was repeated, and the final parameters of Pt−O and first Pt−Pt shell contributions (peak at about 2.8 Å) were obtained by the fitting of the raw data using a nonlinear least square multiple shell fitting routine.[17] The resulting coordination parameters and the corresponding standard deviations are summarized in Table 2 for the fresh electrode and in Table 3 for the used one. The comparisons of the data with the fit, both in k space and in r space, are shown in Figures 8 and 9, respectively, for the fresh and used electrode samples. The number of parameters used to fit the data in this main-shell analysis is 8; the statistically justified number, calculated from the Nyquist theorem,[18] is approximately 16.

According to van Zon,[12] types of backscattering atoms can be identified by corrected Fourier transforms of EXAFS data; peaks which are not symmetrical are a superposition of more than one contribution. Shown in Figure 10, the peaks of the

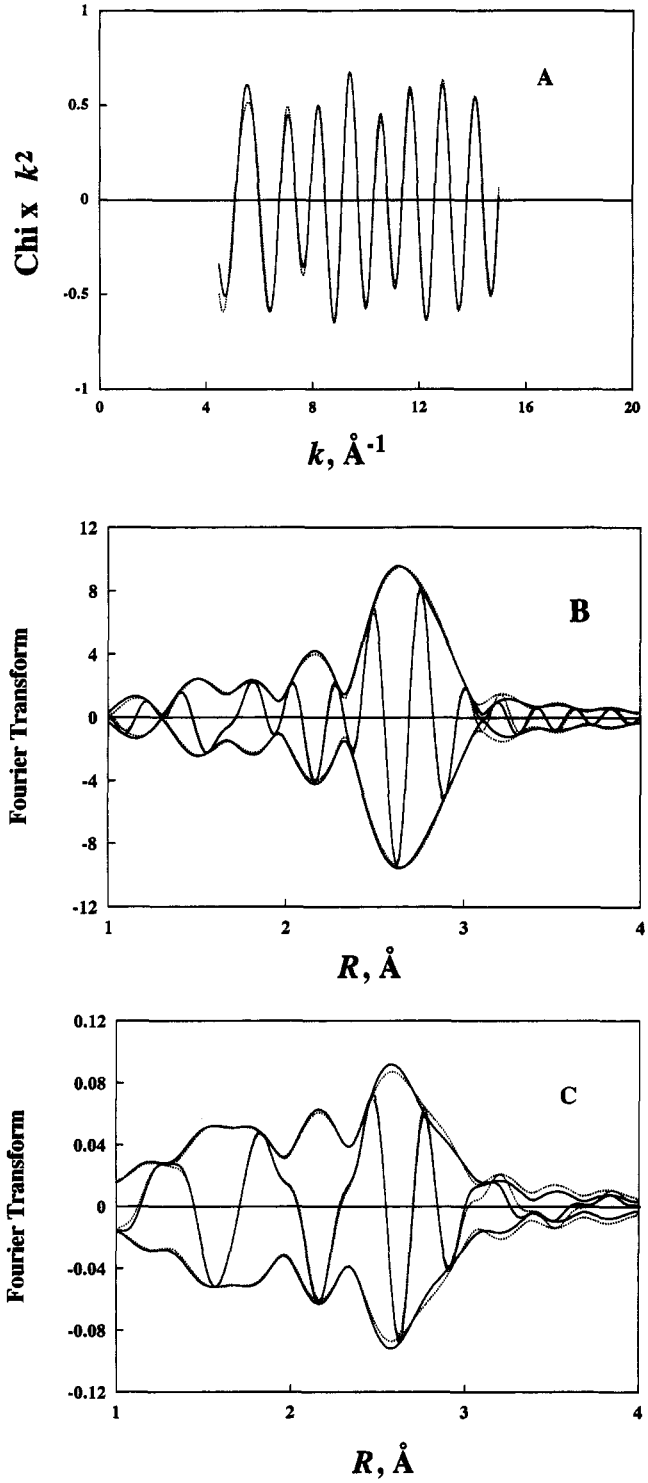

Figure 8. Results of an EXAFS analysis obtained with the best calculated coordination parameters for the fresh electrode (A) k^2-weighted experimental EXAFS data (solid line) and the sum of the calculated Pt−Pt + Pt−O contributions (dotted line), (B) imaginary part and magnitude of Fourier transform (k^3-weighted, Δk = 4.5−15.0 Å) of experimental EXAFS data (solid line) and the sum of the calculated Pt−Pt and Pt−O contributions (dotted line), and (C) Imaginary part and magnitude of Fourier transform (k^1-weighted, Δk = 4.5−15.0 Å) of experimental EXAFS data (solid line) and the sum of the calculated Pt−Pt and Pt−O contributions (dotted line).

Pt−O phase-corrected Fourier transform of the original filtered EXAFS raw data characterizing the fresh electrode sample minus the calculated Pt−Pt contribution are symmetrical. The results thus indicate that no contributions other than Pt−O are significant. The contribution was due to the interaction between Pt and surface hydrous oxide.[5]

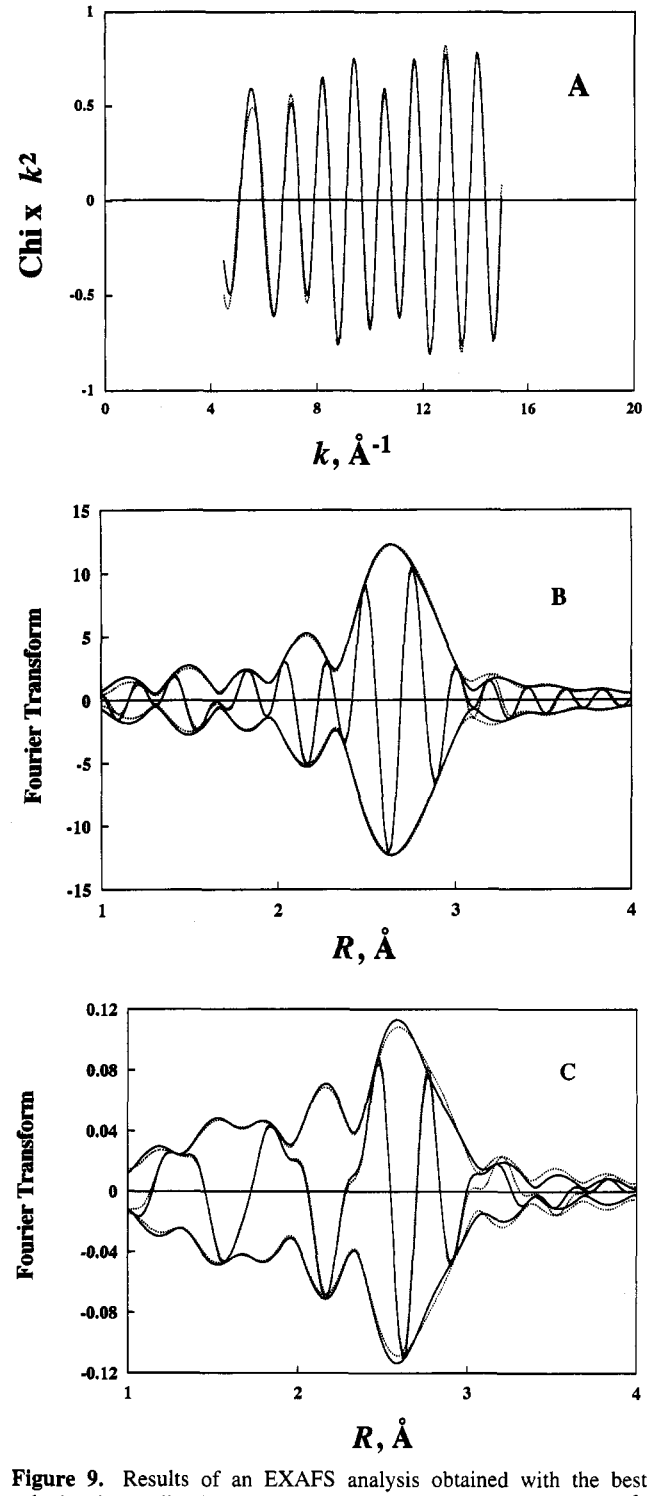

Figure 9. Results of an EXAFS analysis obtained with the best calculated coordination parameters for the used electrode (A) k^2-weighted experimental EXAFS data (solid line) and the sum of the calculated Pt−Pt and Pt−O contributions (dotted line), (B) imaginary part and magnitude of Fourier transform (k^3-weighted, Δk = 4.5−15.0 Å) of experimental EXAFS data (solid line) and the sum of the calculated Pt−Pt and Pt−O contributions (dotted line), and (C) imaginary part and magnitude of Fourier transform (k^1-weighted, Δk = 4.5−15.0 Å) of experimental EXAFS data (solid line) and the sum of the calculated Pt−Pt and Pt−O contributions (dotted line).

For higher Pt−Pt shell analysis, A k^2-weighted Fourier transformation without correction was again performed on the EXAFS function over the range 4.25 < k < 17.47 Å^{-1} for the fresh electrode sample and 4.21 < k < 17.94 Å^{-1} for the used electrode. The total contributions of the main, the second Pt−Pt, and the third Pt−Pt shell were isolated by inverse Fourier transformation of the data in the range 1.15 < r < 5.00 Å for

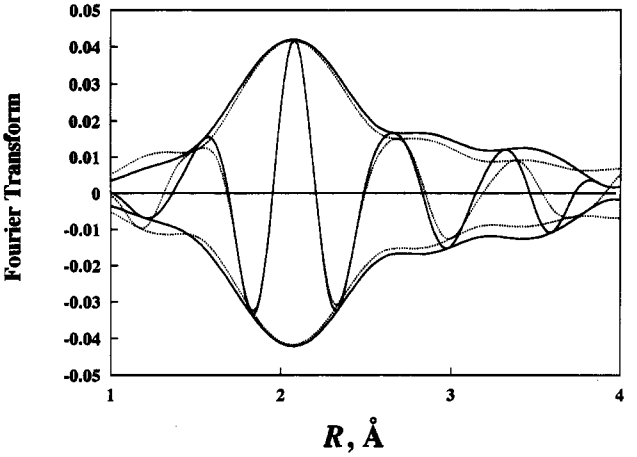

Figure 10. Illustration of the low Z backscattering contributions for the fresh electrode: imaginary part and magnitude of the Fourier transform (k^1-weighted, Pt−O phase corrected, Δk = 4.50−10.0 Å) for raw data minus calculated Pt−Pt EXAFS (solid line) and calculated Pt−O EXAFS (dotted line) contributions.

the fresh electrode sample and $1.08 < r < 5.00$ Å for the used electrode. EXAFS functions calculated from the first Pt−Pt shell and Pt−O coordination parameters were then subtracted from the raw data (Fourier-isolated EXAFS function). Parameters for the higher Pt−Pt shells were determined from the residual spectrum with k ranging from 7.00 to 15.00 Å^{-1}. A straightforward two-shell fit was performed by a nonlinear least square multiple shell fitting routine. First guess of the parameters, N, $\Delta\sigma^2$, and ΔE_0, for this two-shell fit were chosen to be equal to those of the first Pt−Pt shell, and the parameters, R, were chosen to be equal to those determined for the second Pt−Pt and the third Pt−Pt shells in Pt foil by XRD (X-ray diffraction) spectroscopy. Since the difference between the coordination distance in the reference shell and the shells to be analyzed is so large, accurate determination of the actual coordination number in the sample will strongly depend on a correct choice for the mean free path λ. According to van Zon,[12] λ = 6 Å is suitable for the higher Pt−Pt shell analysis. However, the coordination numbers N_{unc} that are determined in the EXAFS analysis will significantly deviate from the actual ones in the samples and need to be corrected by the equation $N = N_{unc}\, e^{2(R_j-R_{ref})/\lambda(k)}$.

The resulting coordination parameters and the corresponding standard deviations for this higher Pt−Pt shell analysis are summarized in Table 2 for the fresh electrode and Table 3 for the used one. The comparisons of the data with the fit in r space are shown in Figures 11 and 12, respectively, for the fresh and used electrode samples.

Morphology of Pt Clusters on the Electrode. The degradation of electrode performance is clearly shown in Figure 13. The declination of cathodic activity in successive cycles with time under the operation conditions of PAFC may be inferred from the failure to maintain Pt dispersion. Pt clusters aggregate during the reaction leading to a decrease of the metal surface and hence the catalytic activity; after six cycles of electrochemical testing the Pt−Pt coordination number increased from 5.5 to 6.1 (Tables 2 and 3). Further information about the structure of these Pt clusters was provided by the higher metal−metal shell contributions. The Pt−Pt bond distance of 3.9 Å (second Pt−Pt shell) is an indication of the three-dimensional character of the metal clusters.[12] For both electrode samples, a small peak was observed in this region (Figure 7), indicating that some three-dimensional metal clusters are present.

The possible morphology of Pt clusters on both fresh and used electrodes is also suggested from the TEM (Figure 2) as

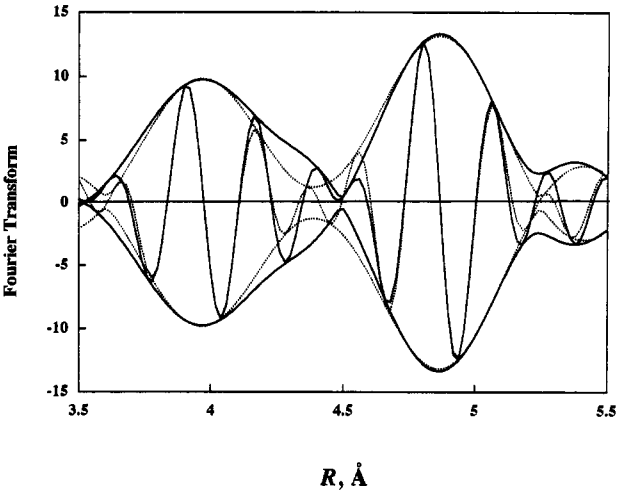

Figure 11. Results of an EXAFS analysis obtained with the best calculated coordination parameters for the isolated higher shells of the fresh electrode: imaginary part and magnitude of the Fourier transform (k^3-weighted, Δk = 4.25−17.47 Å, Pt−Pt phase and amplitude corrected) of experimental EXAFS data (solid line) and the sum of the calculated second Pt−Pt and third Pt−Pt contributions (dotted line).

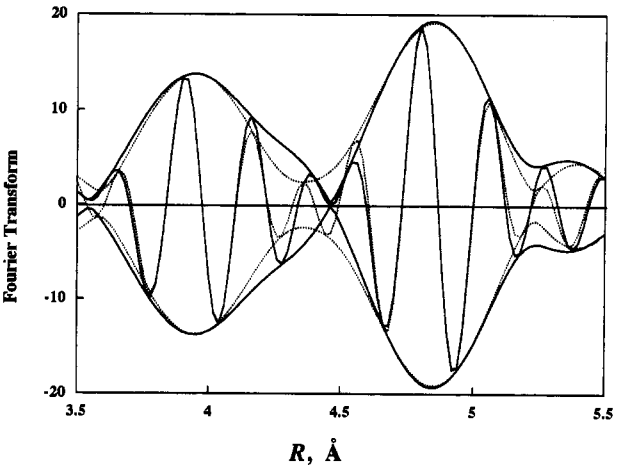

Figure 12. Results of an EXAFS analysis obtained with the best calculated coordination parameters for the isolated higher shells of the used electrode: Imaginary part and magnitude of the Fourier transform (k^3-weighted, Δk = 4.21−17.94 Å, Pt−Pt phase and amplitude corrected) of experimental EXAFS data (solid line) and the sum of the calculated second Pt−Pt and third Pt−Pt contributions (dotted line).

well as the EXAFS results (Tables 2 and 3). The average particle size of the fresh catalyst from TEM is about 32 Å, corresponding to close packed Pt clusters with a coordination number of about 8.5.[19] This number is higher than the 5.5 estimated from the EXAFS function; the only possible explanation for this inconsistency is that not all the Pt clusters on the electrode are spherical or hemispherical in shape; presumably both hemispherical and raft-shaped Pt clusters are present. The proposed morphology of the Pt clusters is simplified, and other models cannot be ruled out. The comparison of the normalized Pt−Pt second shell contribution of Pt foil and the electrodes supports the proposed morphology of Pt clusters; as shown in Figure 14, the normalized Fourier transform peak at about 3.9 Å for both the fresh and used electrodes is lower than that of the Pt foil reference.

Since the EXAFS characteristic peaks for higher Pt−Pt contributions are rather small, the standard deviation of the coordination numbers determined for the second and third Pt−Pt shells (Tables 2 and 3) is relatively high. However, an increase of the second and third Pt−Pt contributions is clearly

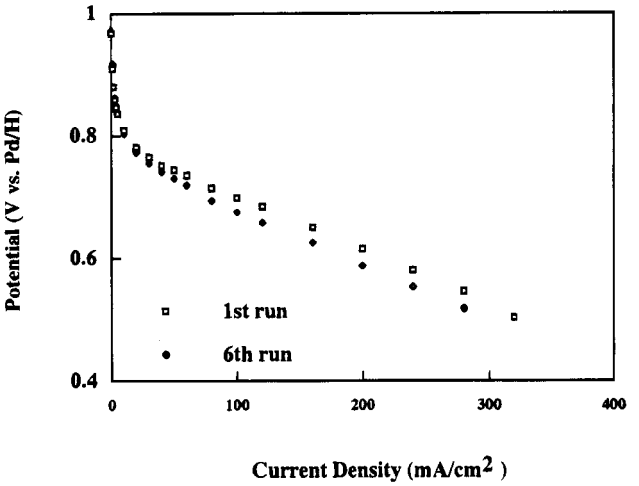

Figure 13. Current vs potential curves for oxygen reduction by using a gas diffusion electrode in phosphoric acid; Pt foil was used as counter electrode, and Pd/H was used as reference electrode; The degradation of the electrode performance was shown by comparison of the first run (squares) and the sixth run (circles).

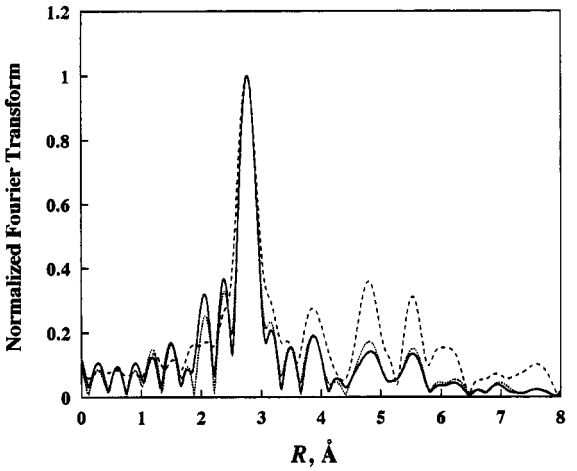

Figure 14. Comparison of the normalized magnitude of the Fourier transform (k^3-weighted, $\Delta k = 3.10-15.0$ Å, Pt−Pt phase and amplitude corrected) of raw EXAFS data at the Pt L_{III} edge between the fresh electrode (solid line), the used electrode (dotted line), and the Pt foil (dash line).

indicated in the increase of the coordination number for these two shells and is also shown in the comparison of Figures 11 and 12. This indicates that the growth of Pt clusters during electrochemical tests occurred in three dimensions. The details of the chemistry whereby the electrochemical tests cause Pt cluster aggregation remain to be elucidated. Our observations and the published results[20] suggest that this Pt cluster aggregation may be due to a combination of the electrochemical reaction, the phosphoric acid, and the temperature. A sintering of Pt clusters in hot phosphoric acid has been observed by Olender et al.[20] The decrease of white line intensity for the used electrode may suggest that the reduction of the oxidized Pt on the electrode is a side reaction of the electrochemical reaction. This reduction reaction may also induce the growth of Pt clusters.

Concerning the durability of the electrocatalysts for the PAFC, a catalyst with higher resistance to the aggregation process is expected to improve the cathodic activity maintenance and hence prolong the fuel cell life. The addition of a second metal is a possible means of inhibiting the metal migration. For the catalytic reforming process, the addition of Re to a γ-alumina-supported Pt catalyst causes dramatic changes in the catalytic behavior of the catalyst, mainly improving the activity maintenance.[21] The Re evidently helps anchor the Pt onto the surface of alumina and maintain it in small ensembles, thus maintaining its activity.[22-25]

Conclusions

X-ray absorption spectroscopy and TEM were used to characterize the structure of Pt clusters on a carbon-supported Pt catalyst, the electrode prepared from that catalyst, and the electrode after six cycles of electrochemical tests. The morphology of Pt clusters was not changed during the process of electrode fabrication. Instead, larger clusters were formed during electrochemical reaction in phosphoric acid electrolyte at 190 °C. Inferred from the correlation between the electrode performance and the structural information characterized by EXAFS and TEM, it is speculated that Pt aggregation is one of the reasons for electrode deterioration.

Acknowledgment. The EXAFS data were analyzed with the XDAP Data Analysis Program, developed by M. Vaarkamp, J. C. Linders, and D. C. Koningsberger, and the reference files were provided by Dr. B. C. Gates. This research was supported by Energy Commission of Minister of Economic Affairs (Grant 843CK1100) and National Science Council of Republic of China (Contract No. NSC 83-0402-E-194-004). We are also grateful to the staff of beam line X-11A at the National Synchrotron Light Source, U.S.A., for their assistance.

References and Notes

(1) O'Grady, W. E.; Taylor, E. J.; Srinivasan, S. *J. Electroanal. Chem.* **1982**, *132*, 137.
(2) Huang, J. C.; Sen, R. K.; Yeager, E. B. *J. Electroanal. Chem.* **1979**, *126*, 768.
(3) Giordano, N.; Pasalacqua, E.; Recupero, V.; Vivaldi, M.; Taylor, E. J.; Wilemski, G. *Electrochim. Acta* **1990**, *35*, 1411.
(4) Sinfelt, J. H.; Via, G. H.; Lytle, F. W. *J. Chem. Phys.* **1978**, *68*, 2009.
(5) Koningsberger, D. C.; Gates, B. C. *Catal. Lett.* **1992**, *14*, 271.
(6) Via, G. H.; Sinfelt, J. H.; Lytle, F. W. *J. Chem. Phys.* **1979**, *71*, 690.
(7) Lagarde, P.; Murata, T.; Vlaic, G.; Freund, E.; Dexpert, H.; Bournonville, J. P. *J. Catal.* **1983**, *84*, 333.
(8) Vaarkamp, M.; Modica, F. S.; Miller, J. T.; Koningsberger, D. C. *J. Catal.* **1993**, *144*, 611.
(9) Vaarkamp, M.; Miller, J. T.; Modica, F. S.; Lanes, G. S.; Koningsberger, D. C. *J. Catal.* **1992**, *138*, 675.
(10) Kawi, S.; Chang, J.-R.; Gates, B. C. *J. Phys. Chem.* **1994**, *98*, 12978.
(11) Watanabe, M.; Tomikawa, M.; Motoo, S. *J. Electroanal. Chem.* **1985**, *182*, 193.
(12) van Zon, J. V. A. D. Ph. D. Dissertation, Eindhoven University of Technology, The Netherlands, 1988.
(13) Lytle, F. W.; Wei, P. S. P.; Greegor, R. B.; Via, G. H.; Sinfelt, J. H. *J. Chem. Phys.* **1979**, *70*, 4849.
(14) Meitzner, G.; Via, G. H.; Lytle, F. W.; Sinfelt, J. H. *J. Chem. Phys.* **1987**, *87*, 6354.
(15) Fung, A. S.; Tooley, P. A.; Kelley, M. J.; Koningsberger, D. C.; Gates, B. C. *J. Phys. Chem.* **1991**, *95*, 225.
(16) Ravenek,W.; Jansen, A. P. J.; van Santen, R. A. *J. Phys. Chem.* **1989**, *93*, 6445.
(17) van Zon, F. B. M.; Maloney, S. D.; Gates, B. C.; Koningsberger, D. C. *J. Am. Chem. Soc.* **1993**, *115*, 10317.
(18) Koningsberger, D. C.; Prins, R. *X-ray Absorption: Principles, Applications, Techniques of EXAFS, SEXAFS and XANES*; Wiley: New York, 1988.
(19) Gates, B. C.; Katzer, J. R.; Schuit, G. C. *Chemistry of Catalytic Process;* McGraw-Hill: New York, 1979.
(20) Olender, H.; O'Grady, W. E.; Isaacs, H. S.; Srinivasan, S. *J. Appl. Electrochem.* **1982**, *12*, 135.
(21) Kluksdahl, H. E. U.S. Patent 3 415 737, 1968.
(22) Purnell, S. K.; Chang, J.-R.; Gates, B. C. *J. Phys. Chem.* **1993**, *97*, 4196.
(23) Sachtler, W. M. H. *J. Mol. Catal.* 1984, *25*, 1.
(24) Shum, V. K.; Butt, J. B.; Sachtler, W. M. H. *J. Catal.* **1985**, *96*, 371.
(25) Shum, V. K.; Butt, J. B.; Sachtler, W. M. H. *J. Catal.* **1986**, *99*, 126.

JP9511109